AiMT Advances in Military Technology
Vol. 6, No. 2, December 2011

Modelling of Ball Impacts on Coatings and Erosion of Special Technique Components

J. Stodola*

Department of Combat and Transport Vehicles, Faculty of Military Technology, University of Defence Brno, Czech Republic

The manuscript was received on 4. February 2011 and was accepted after revision for publication on 4 October 2011.

Abstract:

Special military ground vehicle operate in extreme conditions and require extensive measurements to improve the durability of all systems and materials in their subsystems. Protective coatings usually perform this function with great success. One of the most pressing needs for special vehicle is the development of high performing coatings for erosion protection of engine components (turbine, compressor, turbocharger, intercooler components, etc.). The approach presented in this paper is based on use of computer simulation techniques to model coating behaviour in simulated erosion conditions. Shear stress and equivalent plastic strain at the coating substrate interference were used as criteria describing coating response to particle impact. This article deals with preliminary modelling results, in terms of selecting range of material properties (internal layers thickness and stress or strain) and coating structure.

Keywords:

Wear, erosion, coating, impact, hardness, modelling.

1. Introduction

Erosion of engine compressor blades is a severe problem for vehicle operating in desert areas or use unpaved landing strips, terrain, etc. Damage caused by eroding particles, such as sand, dust or volcanic ash, lowers engine power, decreases fuel efficiency and, in effect, shortens engine service life [1]. Military experience in the Gulf War and Afghanistan demonstrated that engine life could be shortened to a fraction of its designed service life expectancy in these environments. In extreme cases, extensive erosion damage can lead to engine failure [2]. As a protective

* *Corresponding author: Department of Combat and Transport Vehicles, University of Defence Brno, Kounicova Str. 65, 662 10 Brno, Czech Republic, Tel. +420 973 442 278, Fax +420 973 443 384, E-mail jiri.stodola@unob.cz*

measure, complex filtration systems are used to stop eroding particles from entering the engine. Several methods are also employed to improve the erosion resistance of engine compressor components. These methods include thermal processes, e.g. bulk hardening and cryogenic treatment surface such as ion implantation and laser processing, and the use of protective coating. The later appears to be the most cost effective option up to date. In the past, few organizations were involved in the development or production of erosion resistant coating for engines. In recent years however, as the issue of erosion resistance of engine components became more pressing, we can observe renewed interest in this subject, and as a result, more companies are becoming engaged. The driving force behind this development is the potential application of the erosion resistant coatings to military hardware of NATO nations. The leading technology in the development of erosion resistant coating is PVD (Physical Vapour Deposition) with arc, magnetron sputtering and electron beam methods in the forefront. Typically, the PVD coatings, such as nitrides or carbides of transition metals, are much harder than most steels or specialized alloys and have appreciably lower erosion or wear rates. However, the common challenge is to produce relatively thick coatings to provide prolonged protection before the substrate material is exposed. Generally, as coating thickness increases, residual stress reaches the level where further thickness increase becomes impossible. To address this issue, coating deposition procedures need to be optimised taking into account the residual stress of the coating, as proposed in [3]. As practice shows, harder coatings have improved erosion rate see Fig. 1.

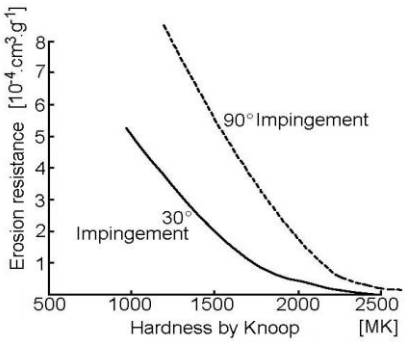

Fig. 1 Erosion resistance of coating

However, very hard coatings are also very brittle and they fail quickly, by fracture and spallation, under repetitive impact load exerted by eroding particles. In erosion test [1], this is evidenced by relatively short lifetime of the coating despite low erosion rate. Extremely hard coatings do not provide required levels of protection the substrate. Obvious solution would be to produce a multi-layered coating combining high hardness and high fracture toughness. In other words, a coating that absorbs most of the impact energy in the top layers and attenuates the stress wave before it reaches the coating substrate interface. In the approach presented in this paper, it was assumed that erosion properties of any erosion resistant coating could be enhanced by designing multi-layered coatings with internal sub microstructures consisting of a number of functional layers of different properties. In the order to understand how the material responds to the impact load, a computer model simulating a particle impact on hard ceramic coatings was developed. The goal of this research was to develop a basic

understanding of the stress and strain distributions within the coating system, with the ultimate objective to develop design principles for new erosion resistant coatings.

2. Erosion Mechanism

Erosion wear is caused by impact of particles of solid or liquid against the surface of an object. Erosive wear occurs in a wide variety of machinery and typical examples are the damage to gas turbine blades and the wear of impellers etc. In common with other mechanisms of wear, mechanical strength does not guarantee wear resistance and a detailed study of material characteristic is required for wear minimization. Properties of the eroding particle are also significant and are being increasingly recognized as a relevant parameter. The term erosive wear refers to an unspecified number of wear mechanisms which occur when relatively small particles impact against mechanical components. This definition is empirical by nature and relates more to practical considerations than any fundamental understanding of wear. The known mechanisms of erosive wear are illustrated in Fig. 2 [4]. The angle of impingement is a very important parameter of erosion and it is the angle between the eroded surface and the trajectory of the particles immediately before impact. A low angle of impingement favours wear processes similar to abrasion because the particles tend to track across the worn surface after impact. A high angle of impingement causes wear mechanisms which are typical erosion. The relationship between wear and impingement angle of ductile and brittle material is shown in Fig. 3. The critical part of modelling erosion properties of a material is establishing the primary erosion mechanism. Erosion by solid particle impact is governed mainly by the velocity of the eroding particles. A comprehensive discussion of impact phenomena in different ranges of particle velocities is given by [5]. In the range of velocities typical for the erosion engines the dominant mechanisms of erosion of the ductile materials (e.g. metals) are plastic fatigue and plastic flow. In the case of brittle materials (e.g. ceramics) brittle fracture and plastic flow dominate. However in any case, individual particle impacts do not cause measurable damage to the target (material removal) and the erosion process progresses only as a result of cumulative damage by multiple impacts. Erosion is a complex process, which is affected by many different factors, such as particle size, shape and mass, impact velocity and angle, mechanical properties of target material, and residual stress in the coating. Analysis of coatings made of several layers is even more complicated because complex mechanical phenomena at the interfaces of separate layers and their interaction with the substrate have to be analysed. Modelling of the dry erosion process has been attempted by many researches using either Monte Carlo simulation or single particle models. Many of these models, despite some simplifying assumptions, produced results that compared well with the experimental results. Though in this work the main interest is in modelling the material response to the impact load, not in the erosion process itself. Hard ceramic coatings, such as TiN, demonstrate typical brittle behaviour in erosion tests. As discussed in [5], the principal erosion mechanism for brittle coatings is brittle fracture. More detailed analysis showed that the morphology of fracture is determined by the extent plastic deformation happening at the point of contact. In the case of either small velocities or rounded particles (e.g. spherical) the contact is essentially elastic and resulting fracture is in the form of axially symmetric cone cracks at the periphery of the contact area. When plastic deformation occurs, which is the case for high velocities or angular (sharp) particles, lateral and radial cracks start from the edge of the plastic zone

around the indentation area. Under actual erosion conditions and under multiple impacts, many types of cracks are produced, which leads to material removal when the cracks interlink and propagate to the free surface. When this happens, small flakes of material are removed from the surface. In the case of thin coatings, cracks may reach the interface and cause local delamination and loss of coating. This also applies to multi-layered coatings.

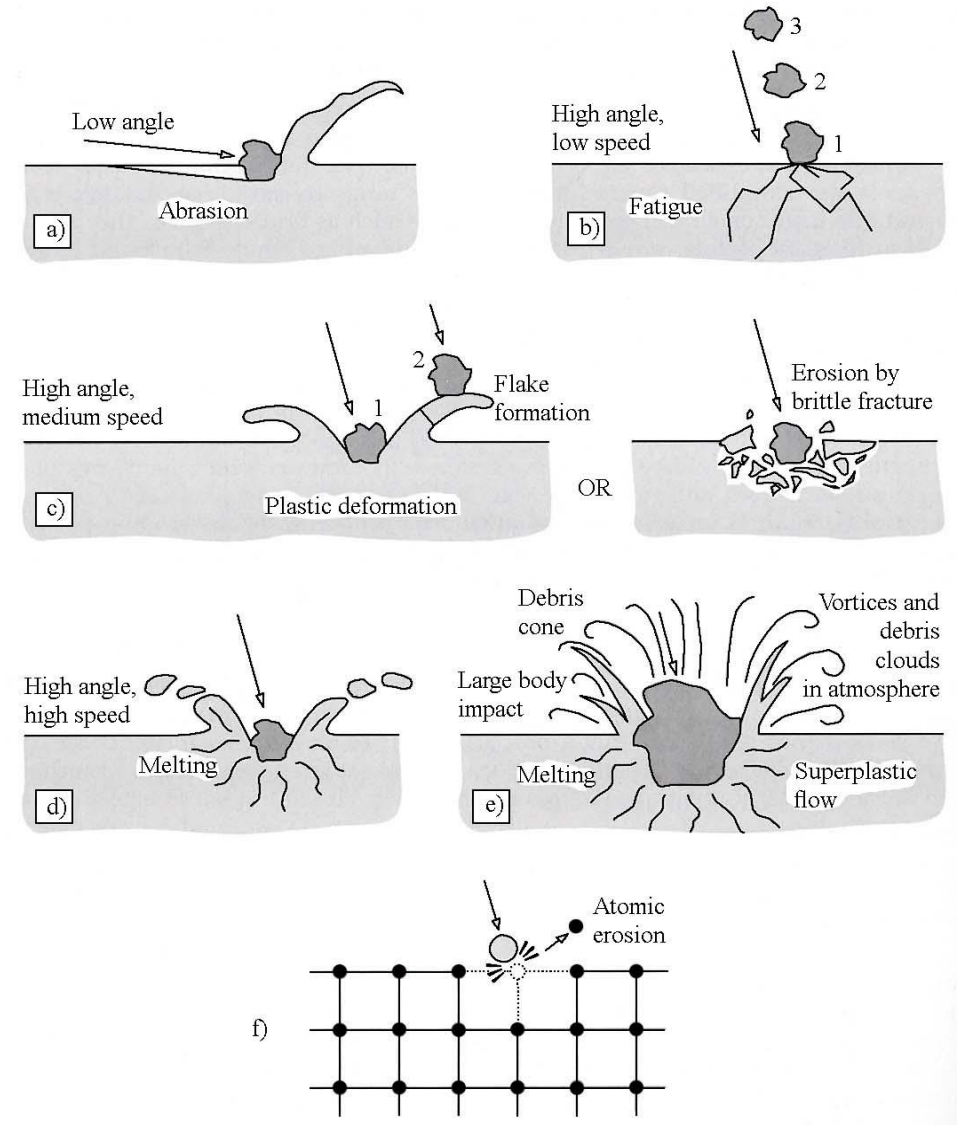

Fig. 2 Mechanisms of erosion: a) abrasion, b) fatigue, c) fracture or plastic deformation, d) melting, e) macroscopic erosion, f) crystal lattice degradation

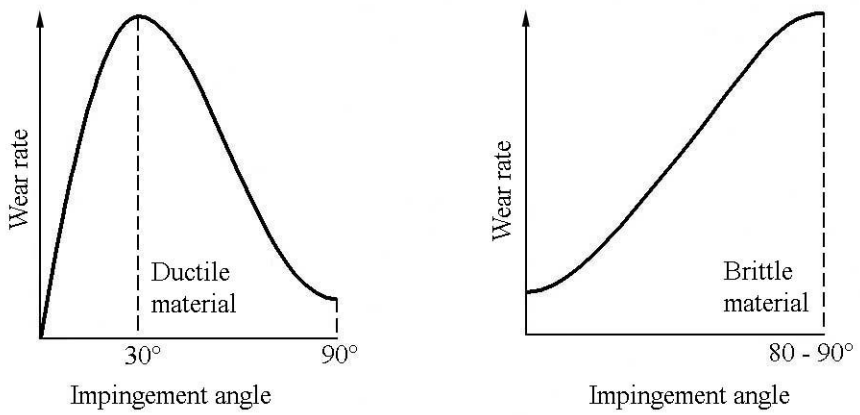

Fig. 3 The effect of impingement angle on wear rates of ductile and brittle materials

Microscopic observations of the erosion scars confirm these mechanisms. From the preceding analysis, it is evident that the erosion properties of the brittle material are defined by the fracture toughness of the material. The cracks nucleate at material defects and propagate if the stress exerted by the impacting particle σ, is greater than the critical value σ_c for the material. The critical stress for crack propagation is given by the equation [6]

$$\sigma_c = \frac{K_C}{\sqrt{\pi \cdot l}} \tag{1}$$

where

K_C … fracture toughness coefficient,

l l … the defect size.

For TiN coating, a coefficient K_C value of 7 MPa·m$^{1/2}$ can be assumed and flow size from 0.1 to 1.0 μm. Under these conditions the critical stress value is between 1.25 and 3.95 GPa. This level of stress (contact pressure) can be produced by a single particle impact [1]. In the case of thin coatings, local delamination under impact occurs when

$$\sigma_c \cdot \sqrt{l} = \frac{K_C(i)}{\sqrt{\pi}} \tag{2}$$

where

$K_C(i)$ … the interfacial fracture toughness.

Interfacial fracture toughness is related to an interfacial energy [6]. Although this parameter is difficult to quantify, it is clearly related to the adhesive strength of the coating. The latter is controlled by the coating deposition process and can be easily measured. In summary, single or multi-layer erosion resistant coating must perform two major functions:

1.) provide a top layer of high hardness and high fracture toughness to delay onset of cracking and minimize erosion rate, and
2.) prevent high stress waves generated by impacting particles from reaching coating or substrate interference and causing delamination.

In the classical approach, many coatings, mostly nitrides or carbides of transition metals, were tried for this moderate success. The main problem was the low fracture toughness of hard coatings. The combination of high hardness and high fracture toughness could not be met by monolithic coatings. The obvious solution was multi-layering of hard and ductile phases in order to increase overall toughness of the coating system. Several such systems, like TiN/Ti, Cr-C/Cr, MO-C/Mo etc. were investigated both experimentally and through finite element method (FEM) [1]. A similar approach was also used to optimise wear resistant coatings. It was demonstrated that multi-layer coatings performed better than their single-layer (monolithic) counterparts although ductile layer thickness needed to be optimised. The second function of the coating is to dissipate the impact energy before it reaches the coating interface and/or to spread it as quickly as possible with high modulus top layers. The latter is a potentially useful concept proposed in [7], for use in composite structures designed to resist ballistic impact. However, applicability of the load spreading concept to erosion resistant coating still needs to be investigated. In this paper, coating properties and layering structure were analysed from the point of view of minimising the damage controlling parameters such as shear stresses appearing at the coating or substrate interface.

3. Energy Balance Model

Finite element modelling of a coating system under particle impact was performed using ordinary software. To analytically verify the numerical calculations a rudimentary model of a rigid ball impacting an elastic target was developed. It was assumed that the ball impacts the target at the right angle. An energy balance method was used to solve the model. To calculate the potential energy of elastic deformation of a target, a Hertzian stress distribution in the contact area was assumed. According to the hertz contact model [8], force acting on a rigid ball during static ball indentation is expressed as

$$F = K_0 \cdot E \cdot D^{1/2} \cdot b^{3/2} \tag{3}$$

where
F … the contact force,
K_0 … the coefficient (0.208),
E … the Young's modulus of the target,
D … the diameter of the ball,
b … the indentation depth.

The elastic potential energy of the delamination can be calculated as

$$E_p = \frac{1}{2} K_0 \cdot E \cdot D^{1/2} \cdot b^{5/2} \tag{4}$$

Subsequently, the kinetic energy of the ball at the time of impact is given by

$$E_k = \frac{1}{2} m \cdot v_0^2 \tag{5}$$

where
m … the mass of the ball,
v_0 … the velocity of the ball at the time of the impact.

In the absence of losses $E_p = E_k$, the maximum indentation of the ball can be calculated as

$$b_{\max} = \sqrt[5]{\frac{m^2 \cdot v_0^4}{K_0^2 \cdot E^2 \cdot D}} \tag{6}$$

As equation (4) describes the non-linear relation between the potential energy and the indentation depth, a linearization of the load indentation equation was required to calculate the time necessary for the impacting ball to indent the target. This linearization was done through an assumption that potential energies of the non-linear and linear systems in the indentation range from 0 to $b_{\max}$ are equal. The linearized expression for elastic potential energy has the following form

$$E_p = E_p^* = \frac{1}{2} k_{eq} \cdot b^2 \tag{7}$$

where

k_{eq} … the linear stiffness of the ball or target system.

A comparison of linearized and non-linearized energies $E_P = E_P^*$ produces the expression for the linearized stiffness

$$k_{eq} = K_0 \cdot E \cdot D^{1/2} \cdot b_{\max}^{1/2} \tag{8}$$

The time required for a ball to fully indent a target may be calculated from equations (5) and (8)

$$t_{imp} = \frac{\pi}{2} \sqrt{\frac{m}{k_{eq}}} \tag{9}$$

The maximum indentation depth (6) and the time (9) were calculated and compared with the numerical results obtained in the FEM calculations. To check the validity of the model a set of initial FEM calculations was performed for a rigid ball impacting a steel substrate with no coating. The displacement of the ball in time was recorded for various substrate properties. An example of the ball displacement in the negative direction of the Y-axis, calculated for the elastic substrate material with no coating and no damping, can be seen in Fig. 4. A steel ball impacting a copper target was modelled using the FEM and the results were compared to calculation results obtained in [9], and to the experimental results obtained in [1]. The steel ball was modelled as a rigid body of 4.8 mm diameter, while the copper target was represented by an axisymmetric body of 10 mm in radius and 5 mm in thickness. The target had elastic-plastic material properties with constant strain hardening coefficient. Material properties for these calculations are presented in Tab. 1.

Tab. 1 Material properties used for testing the FEM [1]

Property	Fe Ball	Cu Target	Units
Young's modulus	203	138	GPa
Poisson's ratio	0.30	0.30	–
Density	7850	8990	kg/m^3
Yield strength	N/A	279	MPa
Tangent modulus	N/A	125.2	MPa

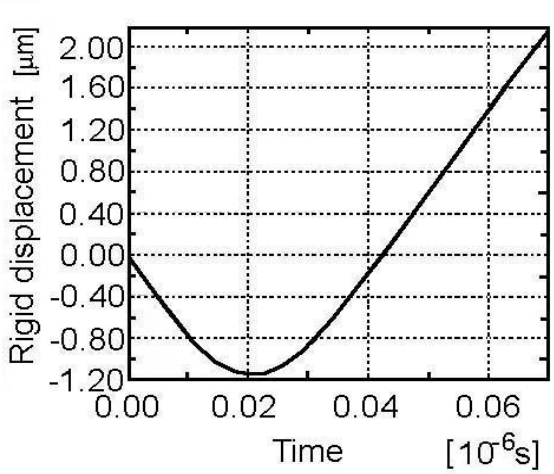

Fig. 4 Results of FEM calculation of rigid ball displacement into a steel target

To compare the numerical results with the experimental ones, depths and radii of the crater created in the target material under three different impact velocities were recorded. Tab. 2 compares measured and calculated crater depths and crater diameters for calculated and experimentally obtained results. Analysis of these results indicates good agreement between calculated and measured results both for the present and in [9] calculations. The differences between calculated results can be attributed to different ball material models, rigid in the present case vs. elastic model in [9].

Tab. 2 Comparison of REM calculation of the size of the impact crater to the experimental results

Impact velocity (m/s)	Crater depth		Difference	Crater radius		Difference
	FEM (mm)	Experiment (mm)	(%)	FEM (mm)	Experiment (mm)	(%)
54.5	0.2812	0.248	11.8	2.242	2.20	1.9
127.5	0.6792	0.626	7.8	3.299	3.20	3.0
198.7	1.1119	1.058	4.8	4.024	3.87	3.8

4. Finite Element Model

For basic understanding of the erosion process for layered systems, a solid mechanics model of particle impacting a hard coating on a substrate was developed using finite element method [1]. Four types of material were used in the model: steel, titanium nitride (TiN), titanium (Ti) and aluminium oxide (Al_2O_3). Several FEMs were prepared to perform calculations of the stress and strains at the interface of the substrate and coating. All models were built using 4-node axisymmetric elements with reduced integration. A typical FEM with a fine mesh that was used for most calculations is shown in Fig. 5.

This model had a radius of 50 μm, which comprised 70 elements. A mesh transition pattern allowed for decreasing the total number of degrees of freedom in the model. Sliding boundary conditions were applied to the nodes along the X and Y axis. The interaction between the rigid ball and the substrate was modelled using special

software [1] in which a contact between a rigid surface and a deformable body with no friction was applied. A constant initial velocity of the ball (77 m/s) was used in all calculations. The relevant material characteristics were assigned to the appropriate finite elements to create required coating or substrate internal structure. The ball radius, mass and velocity were representative of erosion conditions used in accelerated test performed according to a standard procedure. In all FEM [10], it was assumed that considered continuous solid mechanics principles still hold for the range of particle dimensions and coating thicknesses.

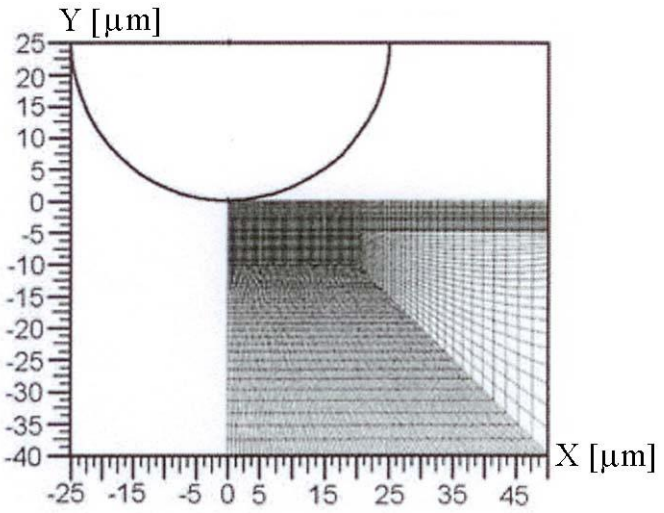

Fig. 5 A typical FEM with a fine mesh

5. Modelling Results

A series of calculations were performed for different thickness of the coating, ranging between 2 and 8 μm, and different values of Young's modulus for the coating, which ranged from 196 to 600 GPa. Equivalent plastic strain in the substrate and the shear stress at the coating or substrate interference were recovered and analysed. Figs. 6 and 7 show typical distributions in time and space of the equivalent plastic strain and shear stresses as the eroding particle impinges the substrate or coating system.

Shear Stress (SS) and Equivalent Plastic Strain (EPS) at the coating-substrate interface were used as an evaluation criterion which describes coating response to a single particle impact. Fig. 8 shows dependence of these parameters on the Young's modulus E_c of the coating. Both parameters were normalized using their respective maximum values obtained for the whole series of calculations.

The larger Young's modulus of the coating, the lower the amount of stress, expressed by shear stress and equivalent plastic strain, that was transmitted to the coating interface. Since a larger Young's modulus usually indicates larger coating hardness a similar relationship may be expected for coating hardness. In the next numerical test, previous calculation for shear stress and equivalent plastic strain were repeated with damping value ($D \neq 0$), i. e. with some level of internal energy loss in the substrate introduced into the computer model. These results are presented in Fig. 9.

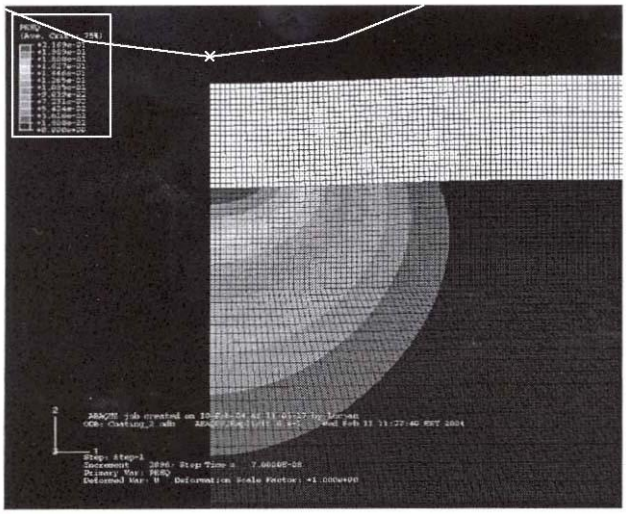

Fig. 6 Equivalent plastic strain distribution in substrate material

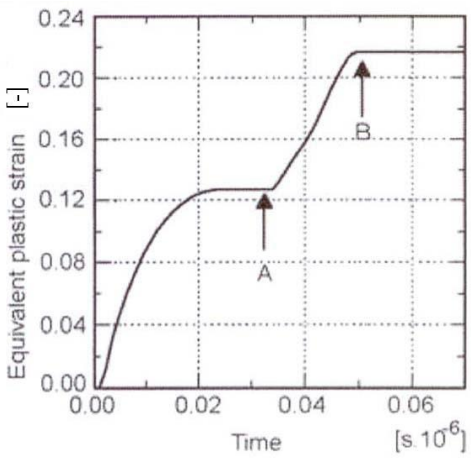

Fig. 7 Development of equivalent plastic strain at the interference in time (A – particle reverses from the maximum depth, B – particle loses contact with the coating)

As shown in Fig. 9, damping lowered the equivalent plastic strain magnitude by approximately 10 %. The damping effect on shear appeared to be smaller by approximately 3 %, but still noteworthy. On the other hand, damping did not change the calculation results qualitatively. Therefore, since calculation times for the cases with damping were much longer, at this stage of model development, damping was not taken further into account. Another characteristic investigated with this model was the effect of the coating thickness. Fig. 10 shows shear stress and equivalent plastic strain dependences for coating ranging in thickness from 2 to 8 μm. The shear stress showed a gradual decrease as coating thickness increased. This correlation may be expected as simple common sense suggests that a thicker coating would be more effective in providing physical separation between the substrate and the surface of the coating where the impact occurs.

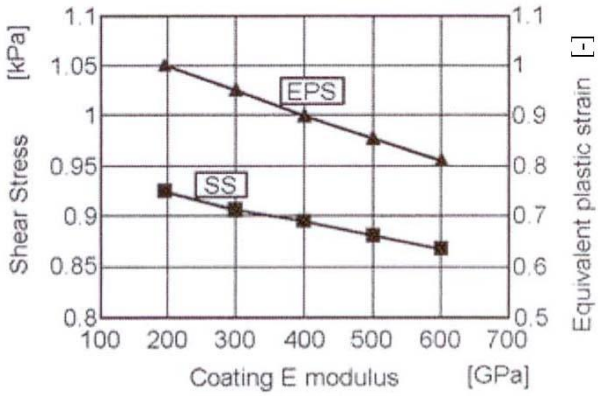

Fig. 8 Shear stress and equivalent plastic strain dependence on Young's modulus of the coating

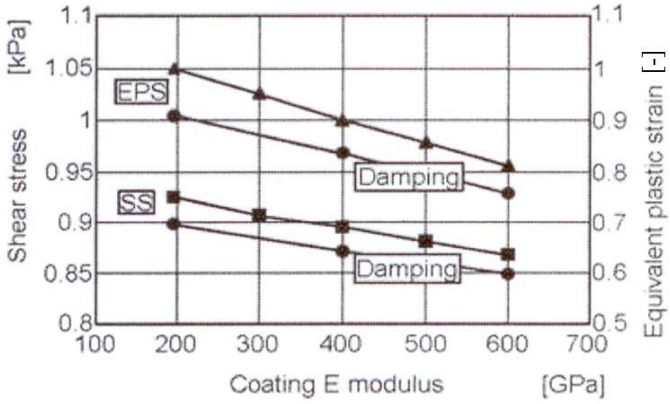

Fig. 9 Effect of damping on shear stress and equivalent plastic strain

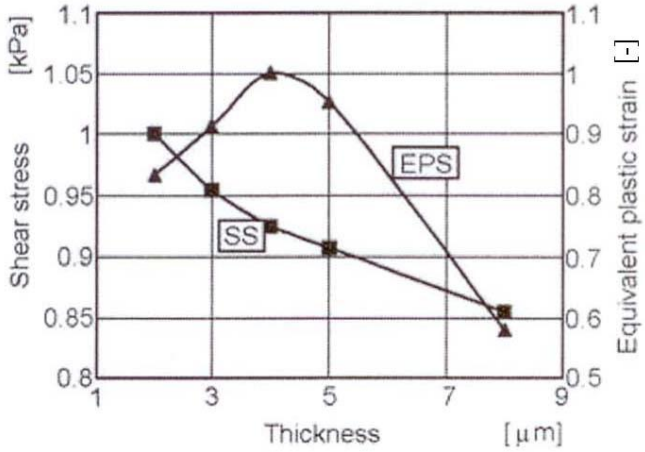

Fig. 10 Effect of coating thickness on shear stress and equivalent plastic strain magnitude at the coating interface

In simplified analyses, one can assume that, for a given coating material, stress wave speed is proportional to the coating modulus. Then, in the absence of internal losses, the results can be interpreted as results of a load spreading by high modulus coatings. The higher modulus of thickness of the coating the more effective load spreading was observed. With the exception of the results in Fig. 11, equivalent plastic strain characteristic showed a similar trend as those for shear stress. However, the equivalent plastic strain curve demonstrated the presence of a local maximum for the 4 μm thick coating. This result can be explained by analyzing the equivalent plastic strain distribution in a radial direction of the model. The equivalent plastic strain distribution vs. true radial distance is shown in Fig. 11. It is evident that for relatively thick coatings the distribution of equivalent plastic strain is bell-shaped. When the coating becomes thinner, the maximum in equivalent plastic strain curve moves off centre, creating a ring of equivalent plastic strain values around the impact centre. This phenomenon is actually observed in experiments. In the case of brittle materials, the edge of the small plastic zone around the impact area is a starting point for radial or lateral cracks. In all cases presented in Fig. 11, larger Young's modulus resulted lower stress at the coating interface, similar to the results presented in Figs. 8 and 9. It means that harder coatings are more resistant to plastic deformation, which again confirms the validity of the computer model.

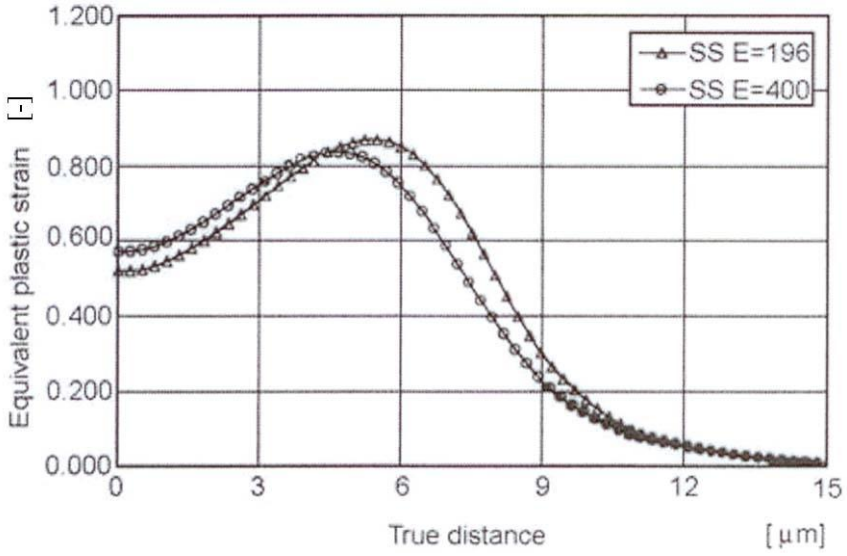

Fig.11 Equivalent plastic strain distribution in radial direction

From the preceding discussion and data presented in Figs 10 and 11, it appears that the shear stress at the coating interface can be effectively used as a single criterion to evaluate coating response to the impact load. Interpretation of equivalent plastic strain data is more difficult since not only maximum value needs to be considered but also the radial distribution. Fig. 12 shows the shear stress dependence on Young's modulus and thickness of the coating.

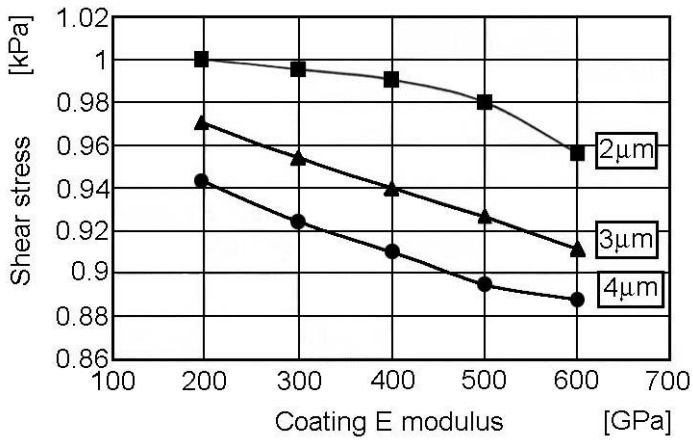

Fig. 12 Shear stress dependence on coating Young's modulus and thickness

Larger Young's modulus and increased coating thickness resulted in lower stress at the coating interface. However, increasing coating hardness and thickness has its practical limits, one of them being residual stress build-up during deposition. Besides, in gas turbine applications coating thickness is limited in order not to affect aerodynamic properties of the blades. Therefore, higher coating performance needs to be achieved by the multi-layering of hard and ductile phases in order to increase overall toughness of the coating system.

6. Conclusion

The modelling results may be considered as extended verification of the computer model rather than a set of coating design principles. However, good qualitative agreement was already obtained with known experimental results and observations. Harder and thicker coatings were found to be more effective in lowering the stress level at the coating or substrate interface. Additionally, coating benefited from the presence of a soft bond layer that contributed to the lowering stresses at the interface and possibly to the increasing of effective fracture toughness of the coating. In quantitative calculations, internal energy losses in the substrate material need to be included. The preliminary modelling results indicate that, in the absence of internal losses, a lower magnitude of stresses at the coating interface can be attributed to the load spreading effect by the high modulus coating materials.

References

[1] BIELAWSKI, M., BERES, W. and PATNAIK, CP. *Modelling of a Single-Particle Impact Response of Erosion-Resistant Coating.* RTO–AVT–109. Paper Nr. 23–1–15, 2004.

[2] PARAMESVARAN, RV et al. *Erosion resistant Coatings for Compressor applications*. Advances in High Temperature Structural Materials and Protective Coatings. Editor Koul, KA. NRC Canada, 1994.

[3] BIELAWSKI, EF. et al. *The Effect of Process Parameters on the Mechanical and Microstructural Properties of Thick TiN Coatings*. Proceedings of the SVC, Dallas, 2004.

[4] STACHOWIAK, WG. and BATCHELOR, WA. *Engineering Tribology*. Third Edition. Elsevier, 2005. 801 p. ISBN 978-0-7506-7836-0.

[5] HUTCHINGS, MI. and FIELD, EJ. *Surface Response to Impact*. Materials at High Strain Rates. Editor Blazynski, TZ. Elsevier, 1987.

[6] OHRING, M. *The Material Science of Thin Films*. Academic Press, 1992.

[7] GUPTA, MY. and DING, LJ. Impact Load Spreading in Layered Materials and Structures: Concept and Quantitative Measure. *International Journal of Impact Engineering*, 2002, vol. 27, no 3, p. 277-291.

[8] JOUNG, CW. *Remark's Formulas for Stress and Strain*. McGraw-Hill, 1989.

[9] WOYTOWITZ, PJ. and RICHMAN, RH. Modelling of Damage from Multiple Impacts by Spherical Particles. *Wear*, 1999, vol. 233-235, p. 120-133.

[10] STODOLA, J. *Advances in Special Technique*. Monograph, 1st Edition. Brno: University of Defence, 2010. 202 p. ISBN 978-80-7231-716-5.

Acknowledgement

This paper was elaborated with the support of the NATO RTA AVT 109 team and partially sponsored by the Ministry of Defence of the Czech Republic within the framework on Research Establishment Development Project.